IOP Conference Series: Materials Science and Engineering

Determination of Burst Pressure of API Steel Pipes using Stress Modified Critical Strain Model

IOP Conf. Series: Materials Science and Engineering **36** (2012) 012025 doi:10.1088/1757-899X/36/1/012025

Determination of Burst Pressure of API Steel Pipes using Stress Modified Critical Strain Model

N. A. Alang[1], N. A. Razak[2] and A.S. Sulaiman[3]
Faculty of Mechanical Engineering, Universiti Malaysia Pahang,
26600 Pekan, Pahang.

E-mail: azuan@ump.edu.my[1], norhaida@ump.edu.my[2], syahrizan@ump.edu.my[3]

Abstract. This paper presents a technique which can be used to determine the burst pressure of defective steel pipes using non-linear finite element (FE) analysis. The technique uses stress modified critical strain (SMCS) failure criterion to study the effect of gouge defects on maximum working pressure of API X65 steel pipes. The procedures in determining the model parameters using 3-D, homogeneous isotropic elastic-plastic material model with large deformation finite element analyses from notched tensile bars were systematically discussed. The relationship between burst pressure and gouge depth was proposed. The burst pressure estimated then was compared to experimental data from the literature for validation showing overall good agreements.

1. Introduction

Various approaches to predict ductile fracture have been proposed in the past. Fracture mechanics, micro-mechanical and cohesive zone models are the main methods that emerged to describe ductile fracture of metals. A micro-mechanical model for ductile fracture, incorporating void nucleation, growth and coalescence, for instance, the Gurson–Tvergaard–Needleman (GTN) model, stress modified critical strain [1], void growth [2], and continuum damage model [3] have been widely used over several decades. As many researchers [1-11] have already published a number of papers using these methods, applicability and validity of these methods have been well discussed. However, few issues need to be resolved in practical application of these methods. For instance, GTN and continuum damage model (CDM) consist of relatively high number of parameters compare to SMCS and void growth model (VGM). Determination and validation of these parameters are not an easy task, and therefore often not reliable.

As recognized by Hancock et al [3], the SMCS model is quite simple since the critical plastic strain as a function of stress triaxiality can be directly calculated and it is not for VGM model where the triaxiality and plastic strain history have to explicitly integrate. Due to its simplicity and accuracy, SMCS model is frequently preferred by researchers to predict the ductile failure of the materials. Mathematically, SMCS model is evaluated by the equation (1):

$$\varepsilon_f = \beta \exp\left(-\frac{3\sigma_m}{2\sigma_e}\right) \qquad (1)$$

where σ_m/σ_e represents stress state triaxiality, ε_f is the true fracture strain and β is a material constant.

[1]Correspondence author: N. A. Alang
Email address: azuan@ump.edu.my

Kanvinde et al [11] compares both VGM and SMCS models in predicting the ductile failure of engineering structural made from structural steels and concludes that both models can be applied accurately to the entire spectrum of structural steels in predicting the failure. Chang et al [8] developed SMCS failure criterion for API X65 steel pipes; widely used for gas pipelines using both smooth and notched tensile bar specimens then applying proposed model to predict the burst pressure of defective pipes using FE analysis and compare the results with experimental results. He reported that the errors are relatively small as less as 5%. However, the study is only limited to constant notch/defect depths and pipe diameters. As the depth of the defects on pipelines increase consistently over the time that mainly due to severity of corrosion [12], the study on its effect is significantly important. In this paper, the local failure criterion namely stress modified critical strain model is applied to predict the burst pressure of defective pipe of API X65 steel. The model was implementing in commercial FE analysis code, MSC PATRAN/MARC. As an extension of Chang et al [8] works, the effect of notch depth on burst pressure for API X65 steel pipes were investigated.

2. Finite Element Analysis

2.1. Materials

The material used in this study was API X65 steel, widely used for gas pipelines. The mechanical properties of the material are tabulated in table 1 [8].

Table 1. Mechanical properties of API X65 steel at room temperature.

Young Modulus, E (GPa)	Poisson Ratio, v	Yield Strength, σ_y (MPa)	Tensile Strength, σ_u (MPa)
210.7	0.3	464.5	563.8

2.2. FE modelling

The test specimens based on Chang et al [8] were used as a model in FE analysis. Detailed dimensions of the test specimens are illustrated in figure 1, showing a round tensile bar with a circumferential notch at the center. In this paper, three different models with notch radius R=1.5, 3 and 6 mm were used. For efficient computation, symmetric conditions are applied. Therefore, all the specimens are modelled in one-four considering symmetry condition. Figure 2 shows the one-four tensile bars with notch radius of 6mm modelled in FE analysis.

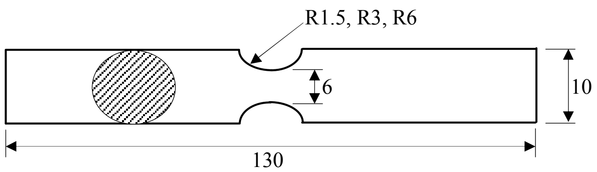

Figure 1. Notched round tensile bars.

Eight node solid elements with reduced integration scheme are applied by using the commercialize MSC PATRAN/MARC software. Based on authors' experiences, there would be little difference of final results by selecting the full integration element and reduced integration element in simulation. The true stress-plastic strain data from Chang et al [10], shown in figure 3, were used as an input in the FE analyses. Materials were modelled as elastic-plastic isotropic homogeneous with large strain/deformation are considered in all cases. Translational constraints are, respectively, imposed on the nodes in the three symmetry plane. The deformation boundary condition was applied to the end of the FE model, and the resulting tensile load was determined from nodal reaction forces.

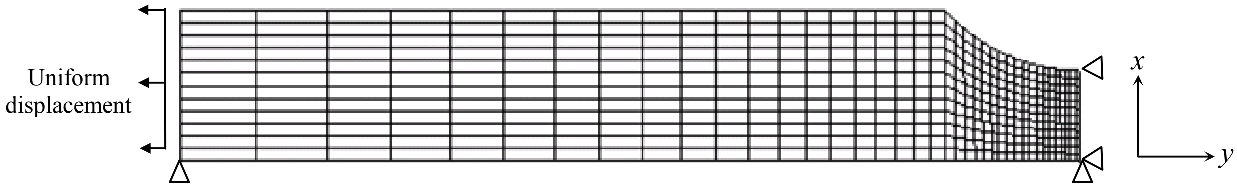

Figure 2. Detailed meshes in 2D views for tensile bars with notch radius of 6 mm.

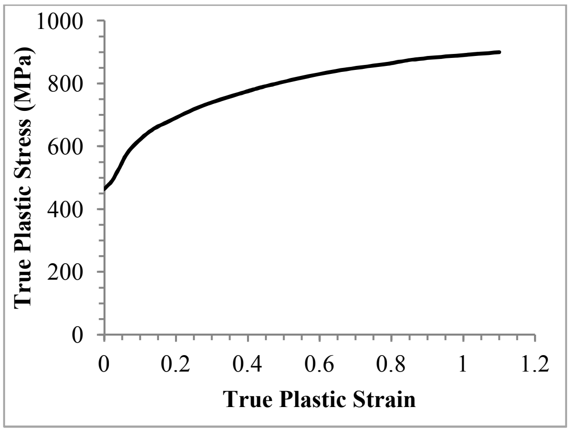

Figure 3. True plastic stress-strain data employed in FE analysis.

2.3. Comparison between FE results and experimental results

Figure 4 shows comparison between experimental engineering stress–strain data from notched tensile bars for notch radius, R=3, and 6 mm with the FE results. It is clearly shown that the FE analysis is able to simulate tensile deformation behaviour even after necking with excellent agreement. However, it cannot simulate the fracture point of tensile test specimens. Therefore, the experimental stress strain data have been compared to simulation results in order to detect the fracture strain of the material. This point was determined at the location where the simulation data divert from one in experiment results.

Figure 5 shows the variation of stress triaxiality and equivalent strain at the minimum section of the bar for three different notch radiuses. Both values are taken at the failure initiation points that have been identified from the previous section (see figure 4). The stress triaxiality, T is defined by the ratio of hydrostatic stress, σ_m and equivalent stress, σ_e and is expressed by:

$$T = \frac{\sigma_m}{\sigma_e} = \frac{\sigma_1+\sigma_2+\sigma_3}{3\sigma_e} \tag{2}$$

The equivalent stress is given by:

$$\sigma_e = \frac{1}{\sqrt{2}}[(\sigma_1-\sigma_2)^2+(\sigma_3-\sigma_1)^2+(\sigma_2-\sigma_3)^2]^{\frac{1}{2}} \tag{3}$$

On the other hand, the equivalent strain σ_e is given by:

$$\varepsilon_e = \frac{\sqrt{2}}{3}[(\varepsilon_1-\varepsilon_2)^2+(\varepsilon_3-\varepsilon_1)^2+(\varepsilon_2-\varepsilon_3)^2]^{\frac{1}{2}} \tag{4}$$

where the σ_1, σ_2, σ_3 and ε_1, ε_2, ε_3 are the principle stresses and principle strain respectively.

It is clearly shown that the stress triaxiality is higher at center of the tensile bar compared to the free surface. Conversely, as seen in figure 5b, the equivalent plastic strain for tensile bar with R=1.5 and 6 mm are higher at free surface than at the bar centre, and the distribution is considerably different for the two notch sizes. However, for tensile bar with R=6 mm, the maximum equivalent plastic strain occurred at the center of the bar. The fact that the effective plastic strain is maximum at the bar surface, whereas fracture initiates at the centre of the bar, emphasizes the significance of stress triaxiality in evaluating fracture initiation.

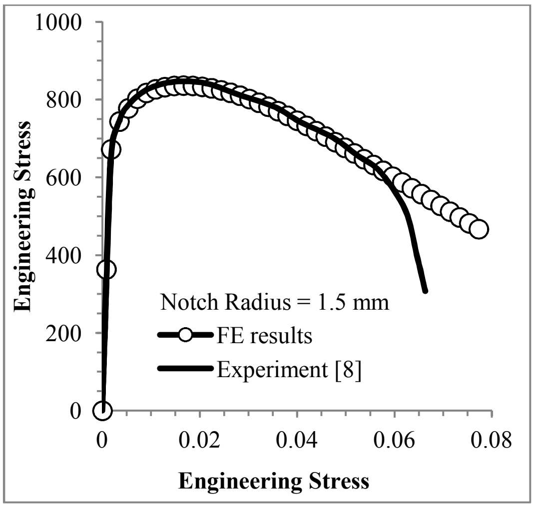

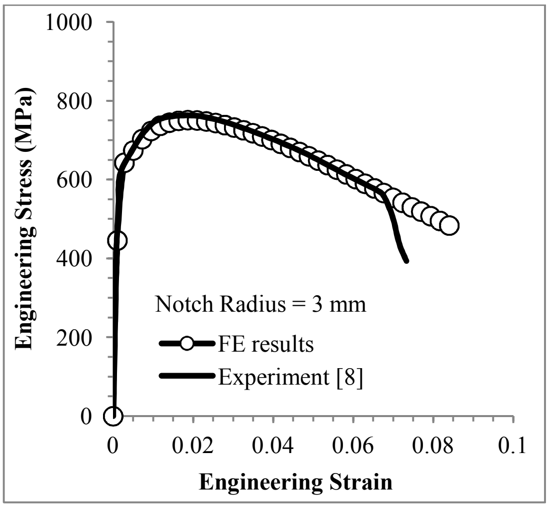

Figure 4. Comparison between experimental and FE results of engineering stress–strain data: (a) notched bar with the 1.5 mm notch radius and, (b) notched bar with the 3 mm notch radius.

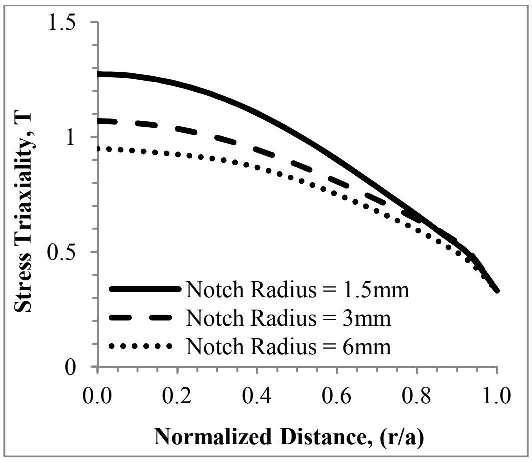

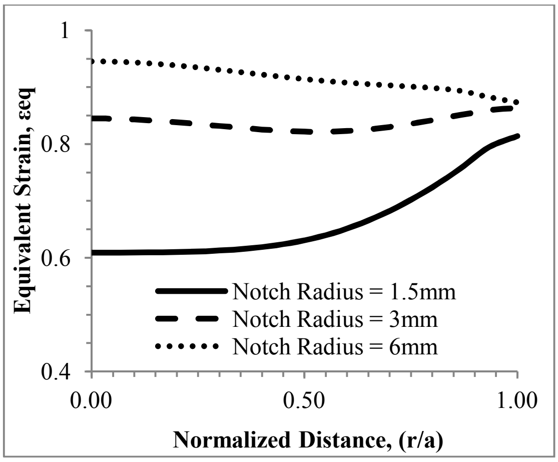

Figure 5. (a) Stress triaxiality profile, (b) equivalent strain profile over minimum cross section.

Figure 6 summarizes the resulting equivalent strain to fracture or true fracture strain, ε_f, as a function of the stress triaxiality for the API steel, considered in the present work. Based on the figure, it is noted that the true fracture strain decreases sharply with increasing of stress triaxiality. The true fracture strain can be represented as an exponentially dependent on the stress triaxiality [1]. Therefore, the following parameters for stress modified critical strain model are proposed:

$$\varepsilon_f = 4.0\exp\left(-1.5\frac{\sigma_m}{\sigma_e}\right) \tag{6}$$

To predict ductile failure of defective pipes made of API X65 steels (considered in present work) using the present approaches, the proposed equation, equation (6) should be combined with detailed elastic-plastic FE analyses from which local stresses and strains are determined. For instance, from the FE analysis, stress and strain information can be monitored as a function of load. Over the loading history, the stress triaxiality and equivalent strain were calculated through equations (3) and (5). Then, the equivalent strain to fracture or true fracture strain is estimated from equation (6). When the equivalent strain from the FE analysis equals the fracture strain, the failure is assumed to occur.

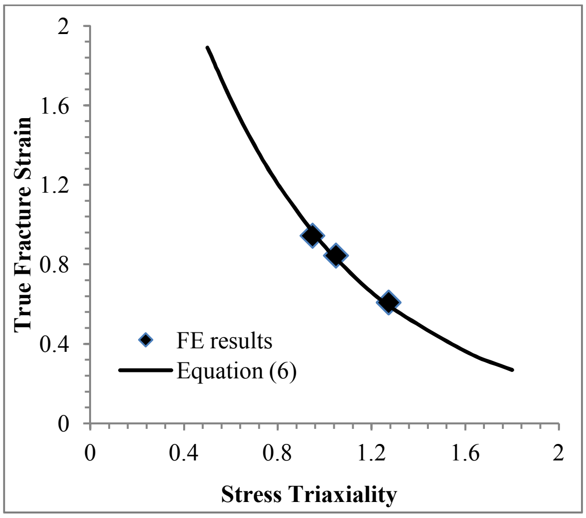

Figure 6. True fracture strain as a function of stress triaxiality

3. Validation

For validation, the burst pressure estimated from FE analysis using proposed model is compared with experimental data from full scale pipe tests [8]. The defective pipe with two different gouge length, l=100mm and 200mm were analyzed. The detailed dimensions of the pipe studied in this paper are according to Chang et al [8]. The pipe has the outside diameter, Do = 762mm, the thickness of t = 17.5mm, and the total length of L =2,300mm. The gouge is characterized by the 45 degree V-notch with the circular notch radius of 2mm. The depth of the gouge is d = 8.75mm which is 50% of the pipe thickness (d/t = 0.5). The pipes with a gouge defect were modelled using MSC PATRAN FE software. A typical finite element mesh is shown in figure 7, with enlargement on the defective region. Internal pressure was applied to the inner surface of the pipe, fixed at one end of the pipe to simulate the closed cap condition and the symmetrical condition was also applied. The results from FE analysis have been compared to experimental data as shown in table 3. The error between these two methods is relatively small therefore increasing the confident on FE analysis.

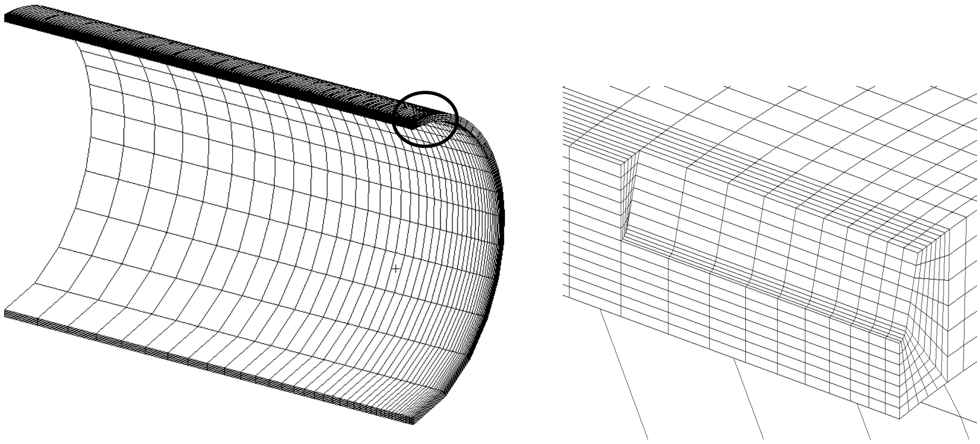

Figure 7. Detailed mesh of the defective pipe used in FE analysis.

Table 3. Comparison of burst pressure between experimental data and FE results.

	Burst Pressure (MPa)	
Gouge Defect	Experiment [8]	FE results Eq. (6)
100mm	24.68	25.8 (4.54%)
200mm	22.48	24.2 (7.65%)

4. Effect of gouge depth on burst pressure

Figure 8 shows schematic illustration of pipe with a gouge on its outer surface. For parametric study, the pipe with different gouge depth is simulated and the burst pressures for each case were predicted. Four gouge depth are chosen for analysis; d = 4.725, 6.563, 8.75 and 13.125 mm.

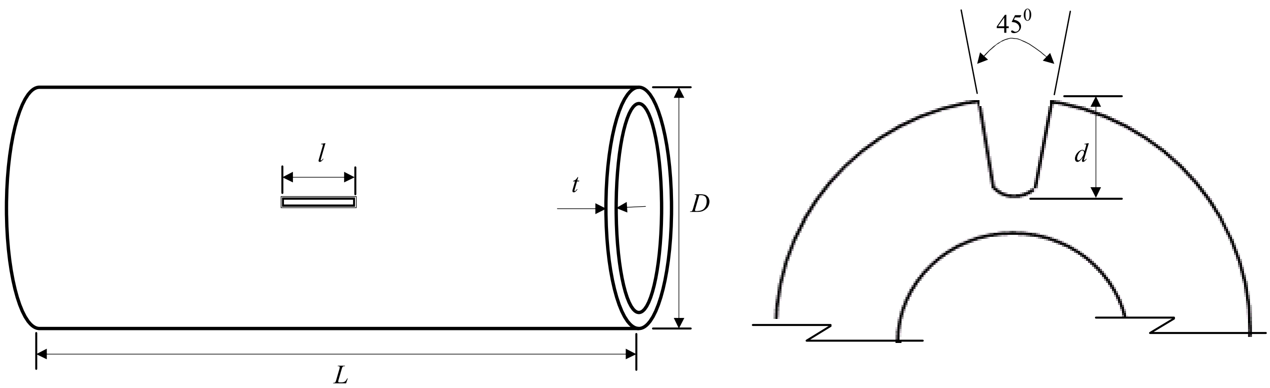

Figure 8. Schematic of pipes with gouge defect.

Shown in figure 9 is a plot of burst pressure versus gouge depth of the pipes in a range of 4.73-13.1 mm. The relationship between two parameters in this range of gouge depth can be represented by linear regression demonstrate a strong correlation. Based on the graph, the burst pressure is strongly dependent on the gouge depth. The burst pressure of the pipe decreases with increasing of gouge depth. Figure 10 shows the variation of pressure as a function of radial displacement taken from the critical location of defective pipes.

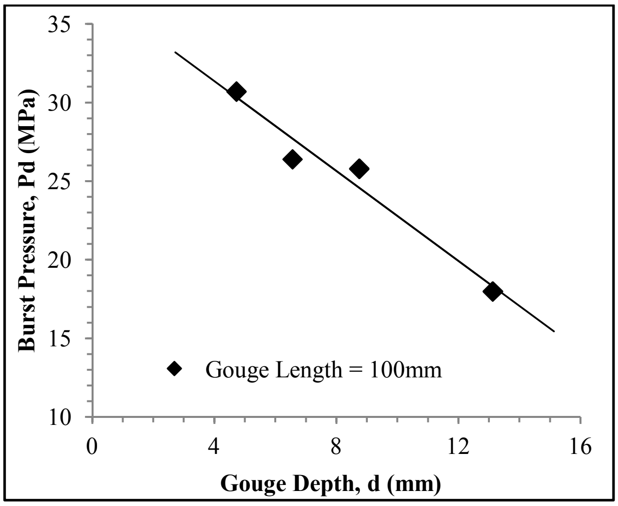

Figure 9. Relationship between burst pressure and gouge depth.

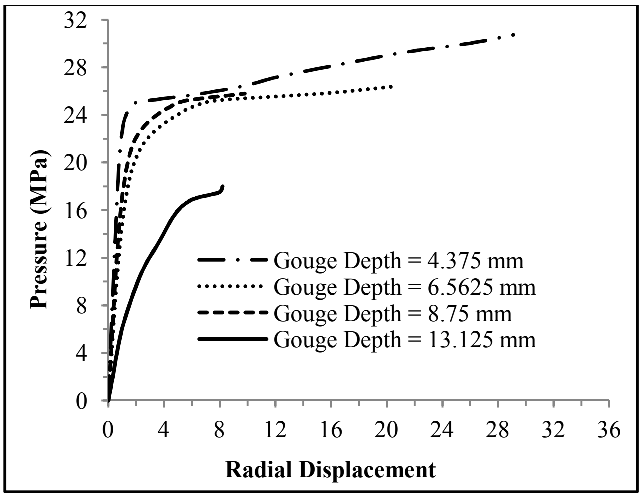

Figure 10. Predicted burst pressure of steel pipes with various gouge depth.

5. Conclusion

In this paper, the burst pressure of defective pipes was estimated using nonlinear FE analysis by implementing the SMCS model. Step by step procedures in determining the model parameters were systematically discussed in this paper. Determination of the parameters of stress-modified critical strain model for given material is quite simple and reliable, as explain in this paper. Using this model, the burst pressure of pipe with different gouge length was predicted and the parametric study of the gouge was also carried out. For validation, API X65 steel (considered in present study) pipes with two different gouge lengths are simulated using FE analysis with the proposed model and the predicted burst pressures are compared with experimental data from literature showing overall good agreements. This study indicates that the burst pressure decreases with increasing of gouge length. Based on parametric study, the relationship between burst pressure and gouge depth for API X65 can be represented by linear regression. In addition, the maximum radial displacement increases with decreasing of gouge depth.

References

[1] Hancock J.W and Mackenzie A.C 1976 On the mechanisms of ductile failure in high-strength steels subjected to multi-axial stress-states *J. Mech. Phys. Solids*. **24** 147-169

[2] Rice J.R and Tracey J 1969 On the ductile enlargement of voids in triaxial stress fields *J. Mech. Phys. Solids*. **17** 201-217

[3] Mackenzie A.C, Hancock J.W and Brown D.K On the influence of state of stress on ductile failure initiation in high strength steels, , *Int J Fract Mech*.

[4] Lemaitre J 1985 A continuous damage mechanics model for ductile fracture *J of Eng Mat and Tech.* **107** 83-89

[5] Bonora N, Gentile D, Pirondi A and Newaz G 2005 Ductile damage evolution under triaxial state of stress: theory and experiments, *Int J of Plasticity*. **21** 981–1007

[6] Zhoua Z, Kuwamura H, Nishida A 2011 Effect of micro voids on stress triaxiality-plastic strain states of notched steels *Procedia Eng.* **10** 1433–1439

[7] Bao Y and Wierzbicki T 2004 On fracture locus in the equivalent strain and strain triaxiality space *Int J of Mech Sciences*. **46** 81-98

[8] Oh C.K, Kim Y.J, Park J.M, Baek J.H and Kim W.S 2007 Development of stress-modified fracture strain for ductile failure of API X65 steel *Int J Fract.* **143** 119–33

[9] Oh C.K, Kim Y.K, Baek J.H and Kim W.S 2011 A finite element ductile failure simulation method using stress-modified fracture strain model *Int J Fract.* **78** 124–137

[10] Oh C.K, Kim Y.J, Baek J.H and Kim W.S 2007 Ductile failure analysis of API X65 pipes with notch-type defects using a local fracture criterion *Int J of Pressure Vessels and Piping.* **84** 512–525

[11] Kanvinde A.M and Deierlein G.G 2005 The void growth model and the stress modified critical strain model to predict ductile fracture in structural steels.

[12] Netto T.A, Ferraz U.S and Estefen S.F 2005 The effect of corrosion defects on the burst pressure of pipelines, *J Constructional Steel Research.* **61** 1185–1204